Development of a Monoclonal Antibody Specific for β/A4 Amyloid in Alzheimer's Disease Brain for Application to In Vivo Imaging of Amyloid Angiopathy

Ronald E. Majocha, John M. Reno, Robert P. Friedland, Christopher VanHaight, Leon R. Lyle and Charles A. Marotta

From the Neurobiology Laboratory, Massachusetts General Hospital, Boston, Massachusetts and the Department of Psychiatry and Neuroscience Program, Harvard Medical School, Boston, Massachusetts; NeoRx Corp., Seattle, Washington; Mallinckrodt Medical, Inc., St. Louis, Missouri; Alzheimer Center, University Hospitals, Cleveland, and Department of Neurology, Case Western Reserve University, Cleveland, Ohio

We evaluated the efficacy of murine monoclonal antibodies (Mabs) targeted to β/A4 amyloid for development of procedures for the in vivo identification of amyloid angiopathy (AA) in Alzheimer's disease (AD). Mabs to β/A4 amyloid were prepared and screened for effectiveness in visualizing AA and senile plaques in postmortem AD brain sections. They were assessed again after enzymatic cleavage to produce Fab fragments and after labeling with ^{99m}Tc using a diamide dimercaptide ligand system. Modified and radiolabeled Fab fragments retained activity and specificity towards amyloid-laden blood vessels and senile plaques. A highly specific murine Mab, 10H3, was identified and characterized that fulfills criteria necessary for the development of a diagnostic imaging agent. Expansion and adaptation of these strategies may provide the methods and materials for the noninvasive analysis of AA in living patients, and permit assessment of the contribution of AA to the clinical and pathological features of AD.

J Nucl Med 1992; 33:2184–2189

The brain circulation is involved in the pathological processes of Alzheimer's disease (AD). Nevertheless, the role of cerebrovascular lesions in the pathophysiology of the disease remains unknown (*1*). Amyloid angiopathy (AA) has been recognized since the early work of Scholz as a significant aspect of the microscopic pathology of AD (*2,3*). Although found to a lesser extent in some healthy older people, AA is severe and common in AD and occurs in greater than 90% of affected brains (*2–7*). The amyloid is readily demonstrated by application of Thioflavin S or Congo red to brain sections (*8–10*). These staining properties reflect the presence of twisted beta fibrils in the vessel wall (*8,11*).

Amyloid infiltration is widespread in the brain microvasculature; affected vessels often pass from the leptomeninges into the cortex. Small cerebral vessels with arterioles that appear as thickened tubes are observed. Involved vessels include small pial and intracortical arterioles, leptomeningeal vessels and, at times, intracortical capillaries, sometimes with destruction of the endothelium (*1,2,13*). Immunocytochemical and electron microscopic studies indicated that the amyloid component of senile plaques often occurs in close proximity to affected microvessels (*12,13*). However, AA may occur without senile plaques (*14*), and the spatial association between plaques and AA may be a chance relationship.

While brain imaging has been widely used in the investigation of AD, presently there are no means to make the diagnosis noninvasively. Furthermore, there are currently no mechanisms for the assessment of the disease's basic pathological features during life in the absence of surgery. The presence of amyloid deposits in small brain vessels in close proximity to the lumen (*13,14*) suggests that an intravenously administered radiolabeled antibody would be capable of in vivo localization. With the goal of developing a highly specific and reactive immunologic probe for AA, a series of studies were carried out on monoclonal antibodies (Mabs) made to a sequence homologous to the β/A4 peptide (*15*). The peptide is the major protein component of amyloid deposits in the AD brain (*15*). We identified and characterized a murine Mab, 10H3, that retains high reactivity and specificity towards AA after a series of modifications required to produce an imaging agent.

Received Jan. 16, 1992; revision accepted Jul. 23, 1992.

For reprints contact: Charles A. Marotta, MD, PhD, Department of Neuroscience and Department of Psychiatry and Human Behavior, Brown University, Box G-M 209, Providence, RI 02912.

MATERIALS AND METHODS

Postmortem Brain

Postmortem brain material was obtained from the Brain Tissue Resource Center at McLean Hospital, Belmont, MA. The brain from an 88-yr-old male with the clinical diagnosis of Familial AD was used for evaluating 10H3. The diagnosis was confirmed upon postmortem examination, which demonstrated the widespread occurrence of senile plaques and neurofibrillary tangles in all brain areas examined. In addition, congophylic angiopathy was noted to involve intraparenchymal vessels as well as vessels within the subarachnoid space. The neurologically normal control brain used in the present study was that of a 65-yr-old male. Brain sections failed to stain with Thioflavin S.

Preparation and Characterization of the Synthetic Amyloid Polypeptide

A 28 residue polypeptide homologous to β/A4 was synthesized by Biosearch (San Rafael, CA). Amino acid analysis verified the structure. The amino acid sequence was reported by Masters and coworkers (*15*) and is here referred to as β/A4(1-28). β/A4(1-28) is homologous, but nonidentical, to the site occupied by amyloid precursor protein (APP) amino acids 597–624 (*16–18*). Peptide samples were stored as a dry powder at −20°C until used.

Immunological Procedures

Immunocytochemistry The preparation of Mab 10H3 was detailed in an earlier report (*10*). Formalin fixed human postmortem brain tissue was kept in 30% sucrose overnight and serially sectioned on a cryostat at 40 μm. After storage in glycerol/water (1:1)-1% sodium azide at −20°C, they were rinsed in Tris-buffered saline (TBST (0.9% NaCl, 20 m*M* Tris, pH 7.4), immersed in 1% H_2O_2 in TBS for 30 min and then rinsed in TBS. Each section was placed in the appropriately diluted primary antibody in immunocytochemistry primary buffer (IPB) (10% goat serum, 2% BSA in TBST [TBS + 0.5% Triton X-100]) overnight. After rinsing with TBST, sections were treated with biotinylated goat anti-mouse IgG [Jackson ImmunoResearch Laboratories, diluted 1:200 in immunocytochemistry secondary buffer (ISB) (2% BSA in TBST)] for 2 hr and then rinsed with TBST. Sections were combined with Avidin DH: biotinylated horseradish peroxidase H complex (Vector) according to the manufacturer's directions, diluted with ISB, rinsed in TBST, developed for 2 min in a diaminobenzidine tetrahydrochloride solution, and mounted and coverslipped.

For the immunofluorescence procedure, the secondary antibody was rhodamine-conjugated goat anti-mouse IgG (Cappel), diluted 1:50, for 1 hr in ISB. Photographs were taken with a Zeiss photomicroscope equipped with the appropriate excitation and barrier filters.

Dot Blots. Fab preparations were characterized on nitrocellulose blots of the starting antigen. Two micrograms of β/A4(1-28) peptide was spotted for each antibody and the latter were tested at concentrations ranging from 0.05 μg/ml to 0.2 μg/ml. The procedures were described in detail earlier (*10*).

Quantitation of Immunostained Plaques

A quantitative assay for antibody specificity was carried out on sections of AD cortex. The numbers of immunostained plaques were counted using a scored grid inserted into the microscope eyepiece. Each grid was 0.25 mm per side; 319 adjacent grids were counted per tissue section for a total area of 19.94 mm^2. Since serial sections were used when comparing antibodies, data from a particular dilution series could be compared within that series with relative certainty that sections contained comparable numbers of plaques.

Antibody Purification

For studies on the purified antibody, the latter was obtained from mouse ascites fluid in a single step using Protein G Sepharose Fast Flow (Pharmacia) following the manufacturers instructions. The purified IgG was characterized by isoelectric focusing as follows. Reagents were obtained from Pharmacia and were applied by means of the general directions supplied by the manufacturer ("Electrophoresis Catalogue").

Antibody Subclass Determination

Isotyping was performed on the purified samples using an ELISA assay for murine IgM, IgG, IgG_2a, and IgG_3 heavy chains and for kappa and lambda light chains. The procedure involved coating a 96 well microtiter plate with GAM (goat anti-mouse) iso-specific capture antibodies (Fisher Biotek) in phosphate buffered saline (PBS) overnight. Any unbound antibodies were removed by washing with 0.5% Tween-20 in PBS. Control and test samples were added at 1 μg/ml in CSPT buffer (5% chicken serum, 0.5% Tween-20 in PBS) and the plates were incubated at 4°C for 1 hr. Unbound antibody was removed by washing with 0.5% Tween-20 in PBS before adding GAM IgG (pan-reactive)-horseradish peroxidase conjugate (Fisher Biotek) and incubated again at 4°C for 1 hr. The microtiter plate as washed again with 0.5% Tween-20 in PBS and a chromogenic substrate (ABTS [2,2′azino-bis(3-ethylbenzthiazoline-6-sulfonic acid] + H_2O_2, Sigma) was added for 30 min at room temperature. Optical densities were recorded on a dual-beam microtiter plate reader set at 415 nm (sample) and 490 nm (reference).

Antibody Fragmentation

Fab fragments of 10H3 were obtained after enzymatic digestion of the whole antibody. Papain bound to agarose beads was obtained from Pierce and activated according to the manufacturer's instructions. 10H3 was exchanged into digestion buffer (0.02 M sodium phosphate, pH 8.5, 0.003 M EDTA, 0.02 *M* L-cysteine, and adjusted to 5 mg/ml). Antibody was mixed with activated papain beads in a ratio of 1 mg of protein per 0.05 ml packed volume of beads. After 18 hr mixing at 37°C, the mixture was centrifuged and the supernatant applied to a 5 ml column of Q Sepharose Fast Flow (Pharmacia) equilibrated with 0.1 *M* sodium phosphate, pH 8.5. The flow-through volume containing pure 10H3 Fab was collected and concentrated to 20 mg/ml. The Fab fragment was pure as judged by SDS-PAGE and gel filtration HPLC.

Radiolabeling of 10H3 Fab with ^{99m}Tc

The Fab fragment was radiolabeled with generator-produced ^{99m}Tc using the diamide dimercaptide bifunctional chelating agent, and procedures, described by Kasina and coworkers (*19*). Briefly, generator produced [^{99m}Tc]pertechnetate was reduced by stannous ion and complexed gluconate ion. The reduced ^{99m}Tc gluconate was added to an acidified solution containing the diamide dimercaptide ligand. The ^{99m}Tc was transchelated into the ligand during a 15 min incubation at 75°C. The ^{99m}Tc ligand solution was cooled to room temperature and adjusted to pH 9.5 with bicarbonate buffer. A solution of antibody in phosphate-

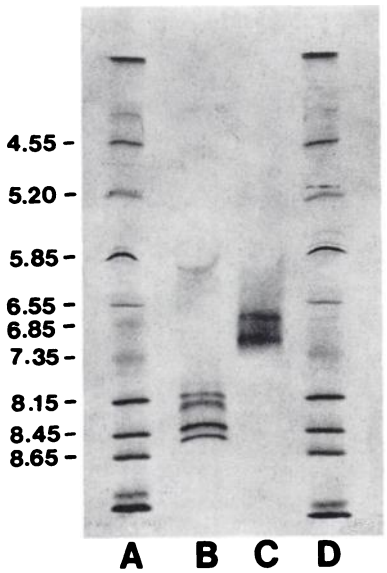

FIGURE 1. Iso-electric focusing gel pattern in 10H3 compared to another unrelated reference antibody (IgG), NR-LU-10. Thelatter is murine in origin and recognizes a 40 Kd glyco-protein expressed by small cell and nonsmall-cell lung carcinoma cells and adenocarcinomas (*34*). Lanes A and D: pH standards. Lane B: 10H3. Lance C: antibody NR-Lu-10.

buffered saline was added to the ^{99m}Tc ligand solution and incubated at room temperature for 20 min. The ^{99m}Tc-labeled antibody was then purified by anion exchange chromatography and diluted with normal saline prior to further use.

RESULTS

Quantitative Immunocytochemistry: Comparative Activity of Mab Preparations

Anti-β/A4 Mabs were prepared and were classified as the gamma 2a kappa isotype. Preliminary screening indicated that Mab 10H3, which had a characteristic isoelectric focusing pattern (Fig. 1), effectively detected senile plaques and amyloid-laden blood vessels of brain parenchyma as well as amyloidotic meningeal vessels of AD brains (Fig. 2A–C). Normal control brains, without amyloid deposits, were unreactive with 10H3 (Fig. 2D) except for light background staining. Quantitative immunocytochemistry was carried out to compare the activity and specificity of 10H3 with othr anti-β/A4 Mabs obtained by the same preparative procedures. Unlike immunostained parenchymal plaques which are comparable in numbers among serial sections of tissue, blood vessels are not uniformly distributed. Thus, quantitation of plaques in adjacent sections served as the basis for immunocytochemical assays. Multiple experiments in which each of several comparable Mabs was tested over a range of concentrations (0.1 μg/ml–10 μg/ml) indicated that 10H3 detected as many or more plaques than other Mabs in the same series at a tenfold greater dilution (Table 1).

Quantitative Immunocytochemistry: Activity After Fab Fragmentation

The Mabs were purified through a protein G column and enzymatically converted to Fab fragments. They re-

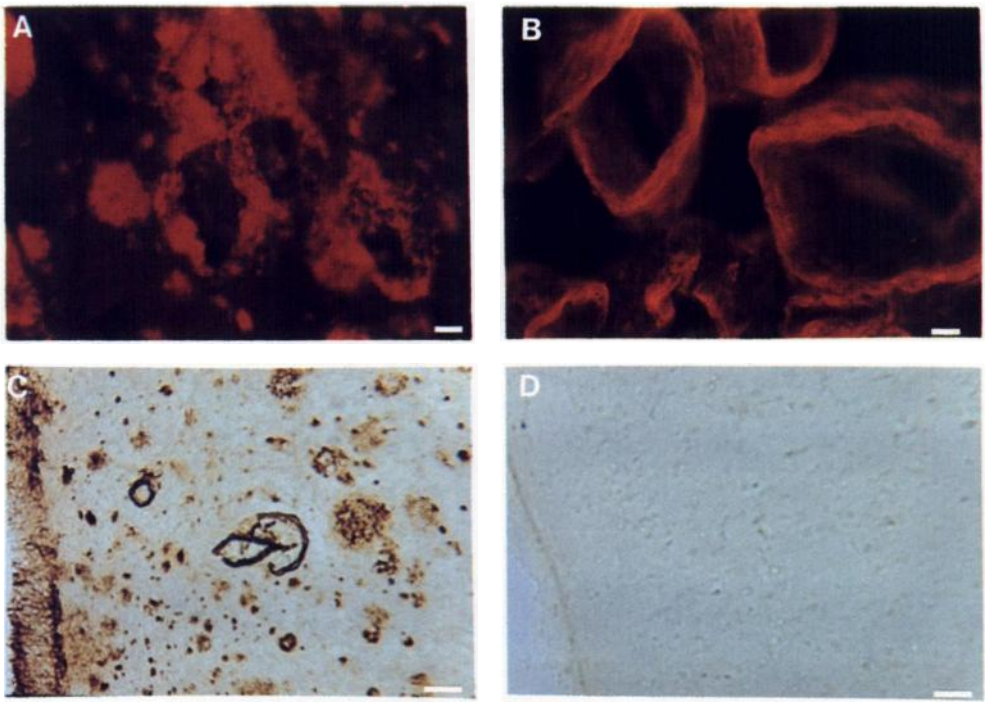

FIGURE 2. Immunostaining of AD brain sections with 10H3 IgG. Sections (40 μm) of a frozen AD brain were cut with a cryostat, mounted on glass slides, and fixed in ice cold ethanol for 15 min. (A and B) Meningeal amyloidotic blood vessels immunostained with fluorescein conjugated goat anti-mouse IgG. (A, bar = 20 μm, B, bar = 10 μm). Further immunostaining utilized the biotinylated horseradish peroxidase complex and diaminobenzidine tetrahydrochloride solution and was carried out on 40 μm frozen brain sections as before. Both the AD brain section shown in panel C and the neurologically normal control shown in panel D were immunostained with the same reagents in simultaneous procedures. In panel C, parenchymal amyloidotic blood vessels and surrounding plaques are clearly visible. (C and D, bar = 50 μm).

TABLE 1
Comparison of Mab Immunoreactivity by Immunohistology*

Mab	Concentration (μg/ml)	Plaques per standard section of AD brain tissue
10H3	1	718
7D10	10	548
5E2	10	310
4E12	10	566

* After testing at various dilutions the Mabs were brought to the indicated concentrations and used to immunostain serial AD brain sections. The number of immunostained plaques determined by the standard assay method are indicated. The area of the stained section was 19.94 mm^2 in each case.

tained 36%–70% activity in the standard immunocytochemistry assay system (Table 2). 10H3 was then assessed relative to other comparable anti-β/A4 Fab fragments by immunocytochemistry. When tested over a range of dilutions found to be effective for processing tissue (0.1 μg/ml–10 μg/ml) 10H3 activity was more effective than other antibodies at one-tenth the concentration (Table 2).

Quantitative/Qualitative Immunocytochemistry: Prelabeled and Postlabeled 10H3

Antibody 10H3 was radiolabeled with ^{99m}Tc using a bifunctional diamide dimercaptide ligand system (see Materials and Methods and Ref. 19). After purification the Fabs were tested for retention of activity. By means of a quantitative dot blot procedure it was shown that the prelabeled and post-labeled Fab fragments each detected as little as 2 μg of antigen at concentration of 0.05 μg/ml (data not shown). Immunocytochemistry carried out at two antibody concentrations indicated that the number of plaques detected by the unmodified Fab fragment were comparable to values for the chelated and radiolabeled species at the effective concentrations (Table 3).

To assess retention of specificity for amyloid accumulations in the AD brain, pre-labeled and post-labeled 10H3

TABLE 2
Comparison of Immunohistological Reactivity After Fab Fragmentation*

Mab	Concentration (μg/ml)	Plaques per standard section of AD brain tissue	Retention of activity (%)
10H3	1	402	56
7D10	10	302	55
5E2	10	212	68
4E12	10	204	36

* After testing at various dilutions, Fab fragments were brought to the indicated concentrations and used to immunostain serial AD brain sections. The numbers of immunostained plaques determined by the standard assay method are indicated. The area of the stained section was 19.94 mm^2 in each case. The percent retention of activity of Fab preparations was calculated based on the data of Table 1.

TABLE 3
Comparison of Immunohistological Reactivity of 10H3 Fab Before and After Radiolabeling with ^{99m}Tc*

	Concentration (μg/ml)	Plaques per standard section of AD brain tissue
Unlabeled	1	224
Labeled	1	261
Unlabeled	5	586
Labeled	5	576

* The number of immunostained plaques determined by the standard assay method are indicated for 10H3 Fab fragments before and after labeling with ^{99m}Tc. See legend to Table 2.

Fab fragments were applied to AD cortex. Both before and after attachment of the diamide dimercaptide chelate of ^{99m}Tc, the Fab exhibited strong affinity for amyloid deposits in blood vessels and parenchyma without a reduction in specificity (Fig. 3).

DISCUSSION

The sequence of the β/A4(1-28) antigen used for preparation of anti-β/A4 antibodies was determined from protein of amyloid plaque cores and shown to have the following sequence: N-Asp-Ala-Glu-Phe-Arg-His-Asp-Ser-Gly-Tyr-Glu-Val-His-His-Gln-Lys-Leu-Val-Phe-Phe-Ala-Glu-Asp-Val-Gly-Ser-Ser-Ala-COOH (*15*). The unique amino acid sequence contains substitutions that distinguish it from AD amyloid peptides obtained by other procedures. When compared with the first 24 residues reported for the corresponding peptide derived from AD brain meninges (*20*) β/A4(1-28) substitutes Glu for Gln at position 11. The β/A4(1-28) sequence also differs from the corresponding strucutre obtained by molecular cloning of APP from nondemented and AD brains (*16,17*); in these cases, β/A4 positions 27 and 28 were occupied by Asn and Lys, rather than by Ser and Ala, respectively.

β/A4(1-28) has the property of aggregating to larger species on denaturing gels (*21,22*). Whereas the calculated mass is 4.2 kD, the β/A4(1-28) sequence self assembles to additional forms that are greater than 23 kD on denaturing acrylamide gels that contain SDS and urea (*21,22*). This characteristic is consistent with the reported behavior of AD amyloid peptides (*23*). By immunoblot procedures 10H3 was shown to react with the immunogen when it occurred both as the 4.2 kD denatured peptide as well as higher molecular weight aggregates (*10,22*).

10H3 and additional anti-β/A4 Mabs reacted with parenchymal deposits of amyloid as well as the amyloid of blood vessels in the AD brain and surrounding meninges. Only pale amorphous background staining of brain tissue occurred in the absence of amyloid deposits in normal control brains. Quantitative immunocytochemistry revealed that 10H3 exhibited greater binding activity than other anti-β/A4 Mabs in the same series. In other studies,

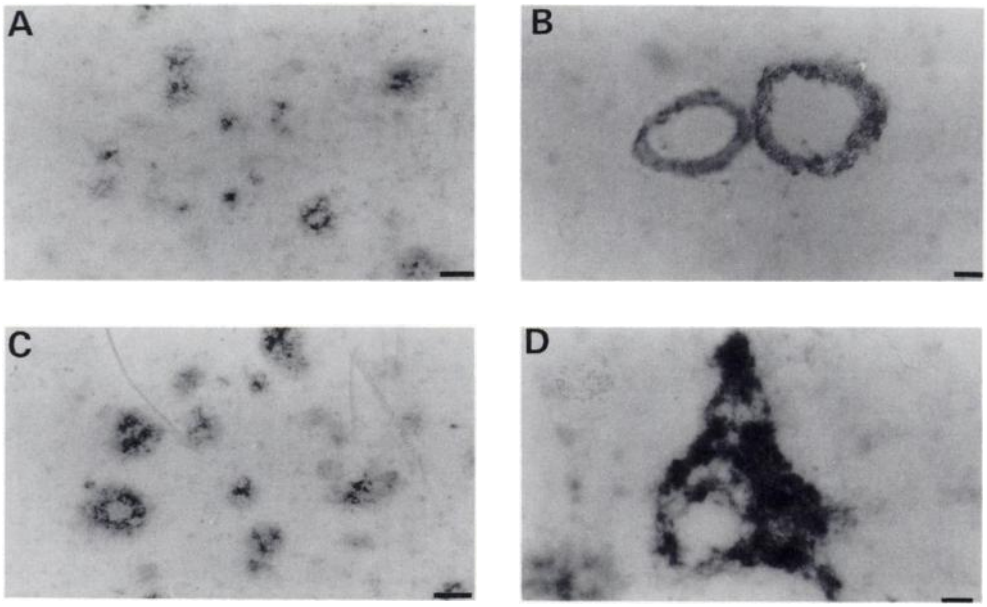

FIGURE 3. Immunostaining of AD brain sections with 10H3 Fab fragments before and after radiolabeling with ^{99m}Tc. Immunostaining is described in the legend to Figure 2. 40 μm AD brain sections were incubated with 1 μg/ml of 10H3 Fab fragments overnight prior to radiolabeling with ^{99m}Tc (A, B) and after radiolabeling with ^{99m}Tc (C, D). Plaque fields are shown in A and C; and amyloidotic blood vessels are shown in B and D. In panels A and C, bars = 20 μm; in panels C and D, bars = 10 μm.

double staining experiments indicated that anti-β/A4 Mabs reacted with plaques and blood vessels that were also detected by thioflavin S but that the Mabs were more sensitive than the dye (*10*).

For radiolabeling of antibodies, Fritzberg and coworkers (*24*) developed a diamide dimercaptide tetradentate chelating agent that allows specific and stable binding of ^{99m}Tc to proteins. The resulting product has a high degree of radiochemical purity and retains its native potency. The novel chelate was used to radiolabel antibodies with ^{99m}Tc for tumor imaging in humans using murine Fab fragments (*25*). The same strategy can be applied to anti-β/A4 Mabs for detection of amyloid angiopathy in the AD brain. It is anticipated that by this approach the diagnosis of AD by brain imaging will be feasible since the radiolabeled antibody retains high affinity and specificity for vascular amyloid, as well as for plaques. This noninvasive imaging technique may provide a means to determine the relationship of imaging evidence for AA to disease course.

While brain imaging has been a subject of extensive investigation in AD (*26,27 et op. cit.*), a noninvasive diagnostic method awaits development. There are currently no approaches to the assessment of the basic pathological features of the disease during life without surgical intervention. By contrast Mabs have been widely used in the imaging and treatment of cancer (*24,28–33*) wherein they provide specific nontoxic markers that were shown to be safe, and, in some settings, more sensitive for tumor detection than other imaging methods. Although radioimmunodetection investigations of brain tumors in humans have been ongoing for more than 25 yr, brain diseases have received limited attention with this technique.

Our current approach takes advantage of the rapid clearance of the Fab fragment of the anti-β/A4 10H3 Mab and the exemplary properties of the ^{99m}Tc label as a diagnostic radiopharmaceutical. If successful targeting occurs, SPECT imaging may provide a noninvasive measure of AA. Localization to intravascular β/A4 deposits is expected to be less prominent in healthy aged control subjects than in AD patients. A radioimmunodetection approach may allow us to assess this hypothesis, as well as attempt to correlate the severity of AA with the severity and duration of illness.

SUMMARY

10H3 is a murine Mab to the AD β/A4 amyloid that is highly reactive and specific for blood vessel and parenchymal amyloid deposits. The Mab retained its binding characteristics after cleavage to a Fab fragment and chelation to a diamide dimercaptide tetradentate agent and labeling with ^{99m}Tc. Based upon these properties the radiolabeled anti-amyloid Fab appears to be a potentially effective agent for application to the diagnosis of Alzheimer disease by in vivo imaging.

ACKNOWLEDGMENTS

Supported in part by the following: Mallinckrodt Medical, Inc. grant award, NIH P01 AG02126 and a Metropolitan Life Foundation Award to C.A.M.; and by NIH grant AG08012 to R.P.F. The authors thank Tressa Dodd and Becky Bottino for their assistance in completing this manuscript.

REFERENCES

1. Friedland RP. The cerebral circulation and the mechanisms of Alzheimer's disease. In: Hayaishi O, Seegmiller JE, Nagatsu T, eds. *Aging of the brain: cellular and molecular aspects of brain aging and Alzheimer's disease. Proceedings of the thirteenth taniguchi symposium.* Tokyo: Japan Scientific Societies Press and Basel: Karger. 1990:147–159.
2. Scholz W. Studien zur pathologie der hirngefasse. II. Die drusige entartung der hirnarterien und capillaren. *Zeit Neurol Psychiat* 1938;162:694–715.
3. Vinters HV. Cerebral amyloid angiopathy: a critical review. *Stroke*

1987;18:311–324.
4. Glenner GG, Henry JH, Fujihara S. Congophilic angiopathy in the pathogenesis of Alzheimer's degeneration. *Ann Pathol* 1981;1:120–129.
6. Ranalli P, Bergeron C. Amyloid angiopathy in Alzheimer's disease. *Ann Neurol* 1984;16:119–127.
7. Ishii N, Ishihara Y, Horie A. Amyloid angiopathy and lobar cerebral hemorrhage. *J Neurol Neurosurg Psychiatry* 1984;47:1703–1011.
8. Glenner GG. Amyloid deposits and amyloidosis. The beta-fibrilloses. I. *N Engl J Med* 1980;302:1283–1292.
9. Allsop D, Landon M, Kidd M, Lowe JS, Reynolds GP, Gardner A. Monoclonal antibodies raised agaisnt a subsequence of senile plaque core protein react with plaque cores, plaque periphery, and cerebrovascular amyloid in Alzheimer's disease. *Neurosci Lett* 1986;68:252–256.
10. Majocha RE, Benes FM, Reifel JL, Marotta CA. Laminar-specific infrastructural diversity of cortical amyloid demonstrated by computer-enhanced imaging of unique epitopes in Alzheimer's disease. *Proc Natl Acad Sci USA* 1988;85:6182–6186.
11. Lee SS, Stemmerman GN. Congophilic angiopathy and cerebral hemorrhage. *Arch Pathol Lab Med* 1978;102:317–328.
12. Mandybur TI. The incidence of cerebral amyloid angiopathy in Alzheimer's disease. *Neurology* 1975;25:120–126.
13. Tomlinson BE, Corsellis JAN. Aging and dementias. In: Adams JH, Corsellis JAN, Duchen LW, eds. *Greenfield's neuropathology,* 4th edition. New York: J. Wiley and Sons, 1984:968–969.
14. Montjoy CQ, Tomlinson BE, Gibson PH. Amyloid and senile plaques and cerebral blood vessles. A semi-quantitative investigation of a possible relationship. *J Neurol Sci* 1982;57:89–103.
15. Masters CL, Simms G, Weinman NA, et al. Amyloid plaque core protein in Alzheimer's disease and Down syndrome. *Proc Natl Acad Sci USA* 1985;82:4245–4249.
16. Kang J, Lemaire JG, Unterbeck A, Salbaum JM, et al. The precursor of Alzheimer's disease amyloid A4 protein resembles a cell-surface receptor. *Nature* 1987;325:733–736.
17. Zain SB, Salim M, Chou WG, Sajdel-Sulkowska EM, et al. Molecular cloning of amyloid cDNA derived from mRNA of the Alzheimer brain. Coding and non-coding regions of the fetal precursor MRNA are expressed in the Alzheimer cortex. *Proc Natl Acad Sci USA* 1988;85:929–933.
18. Chou W-G, Majocha RE, Sajdel-Sulkowska EM, et al. Immunologic and molecular genetic studies on amyloid deposition in the Alzheimer's disease brain. *Brain Dysfunction* 1988;1:133–145.
19. Kasina S, Rao TN, Srinivasan A, Sanderson JA, et al. Development and biologic evaluation of a kit for preformed chelate technetium-99m radiolabeling of an antibody Fab fragment using a diamide dimercaptide chelating agent. *J Nucl Med* 1991;32:1445–1451.
20. Glenner GG, Wong CW. Alzheimer's disease: initial report of the purification and characterization of a novel cerebrovascular amyloid protein. *Biochem Biophys Res Commun* 1984;120:885–890.
21. Salim M, Zain SB, Chou WG, et al. Molecular cloning of amyloid cDNA from Alzheimer brain messenger RNA. Correlative neuro-immunologic and in situ hybridization studies. In: Blass JP, Miner GD, Miner LA, Richter RW, Valentine JL, eds. *Familial Alzheimer's disease: molecular genetics, clinical prospects and societal issues.* New York: Marcel Dekker; 1988:153–165.
22. Honda T, Marotta CA. Arginine specific endopeptidases modify the aggregation properties of a synthetic peptide derived from Alzheimer β/A4 amyloid. *Neurochem Res* 1992;17:367–374.
23. Gorevic PD, Castano EM, Sarma S, Frangione B. Ten to fourteen residue peptides of Alzheimer's disease protein are sufficient for amyloid fibril formation and its characteristic x-ray diffraction pattern. *Biochem Biophys Res Commun* 1987;147:854–862.
24. Fritzberg AR, Kasina S, Reno JM, Srinivasa A, et al. Radiolabeling of antibodies with Tc-99m using N_2S_2 ligands. *J Nucl Med* 1986;27:957–958.
25. Eary JR, Schroff W, Abrams PG, Fritzberg AR, et al. Successful imaging of malignant melanoma with technetium-99m-labeled monoclonal antibodies. *J Nucl Med* 1989;30:25–32.
26. Friedland RP. Brain imaging and cerebral metabolism. In: Boller F, Grafoxen J, eds. *Handbook of neuropsychology, volume 4.* Amsterdam: Elsevier, 1990:197–212.
27. Friedland RP, Budinger TF, Ganz E, et al. Regional cerebral metabolic alterations in dementia of the Alzheimer-type: positron emission tomography with 18-fluorodeoxyglucose. *J Comp Assist Tomogr* 1983;7:580–589.
28. Carrasquillo JA, Krohn KA, Beaumier P, et al. Diagnosis of and therapy for solid tumors with radiolabeled antibodies and immune fragments. *Cancer Treat Rep* 1984;68:317–328.
29. Sands H. Radiolabeled monoclonal antibodies for cancer therapy and diagnosis: is it really a chimera? *J Nucl Med* 1987;33:29–32.
30. Divgi CR, Welt S, Kris M, et al. Phase I and imaging trial of 111-labeled anti-epidermal growth factor receptor monoclonal antibody 225 in patients with squamous cell lung carcinoma. *J Neurosurg* 1987;67:721–725.
31. Blasberg RG, Makagawa H, Burdon MA, Groothuis DR, Patlak CS, Bigner DD. Regional localization of a glioma-associated antigen defined by monoclonal antibody 81C6 in vivo: kinetics and implications for diagnosis and therapy. *Cancer Res* 1987;47:4432–4443.
32. Fujimori K, Covell DG, Fletcher JE, Weinstein JN. A modeling analysis of monoclonal antibody percolation through tumors: a binding-site barrier. *J Nucl Med* 1990;31:1191–1198.
33. Wilbur DS, Hadley SW, Hylarides MD, et al. Development of a stable radioiodinating reagent to label monoclonal antibodies for radiotherapy of cancer. *J Nucl Med* 1989;30:216–226.
34. Morris JF, Krishnamurthy S, Antoniovic R, Duncan C, Turner FE, Krishnamurthy GT. Technetium-99m monoclonal antibody fragment (Fab) scintigraphy in the evaluation of small cell lung cancer. *Nucl Med Biol* 1991;18:613–623.